

Similarities and Differences Between Cyclodextrin–Sodium Dodecyl Sulfate Host–Guest Complexes of Different Stoichiometries: Molecular Dynamics Simulations at Several Temperatures

Pilar Brocos,[†] Norma Díaz-Vergara,^{‡,§} Xavier Banquy,^{‡,||} Silvia Pérez-Casas,[‡] Miguel Costas,[‡] and Ángel Piñeiro^{*,†,‡}

Departamento de Física Aplicada, Facultad de Física, Universidad de Santiago de Compostela, Campus Vida, E-15782 Santiago de Compostela, Spain, and Laboratorio de Biofisicoquímica, Departamento de Fisicoquímica, Facultad de Química, Universidad Nacional Autónoma de México, Cd. Universitaria, México D.F. 04510, Mexico

Received: April 10, 2010; Revised Manuscript Received: August 17, 2010

An extensive dynamic and structural characterization of the supramolecular complexes that can be formed by mixing α -, β -, and γ -cyclodextrin (CD) with sodium dodecyl sulfate (SDS) in water at 283, 298, and 323 K was performed by means of computational molecular dynamics simulations. For each CD at the three temperatures, seven different initial conformations were used, generating a total of 63 trajectories. The observed stoichiometries, intermolecular distances, and relative orientation of the individual molecules in the complexes, as well as the most important interactions which contribute to their stability and the role of the solvent water molecules were studied in detail, revealing clear differences and similarities between the three CDs. Earlier reported findings in the inclusion complexes field are also discussed in the context of the present results. For any of the three native cyclodextrins, the CD_2SDS_1 species in the head-to-head conformation appears to be a promising building block for nanotubular aggregates both in the bulk and at the solution/air interface, as earlier suggested for the case of α -CD. Moreover, the observed noninclusion arrangements involving β -CD are proposed as the seed for the premicellar (β -CD)-induced aggregation of SDS described in the literature.

1. Introduction

Natural cyclodextrins (CDs) are cyclic oligosaccharides formed by six (α), seven (β), or eight (γ) α -1,4-linked α -D-glucopyranoside units (GPUs) that result from the enzymatic degradation of starch. Their structure has been described as truncated cone shaped with a hydrophobic cavity and a hydrophilic outside that makes them relatively soluble in water. The primary and secondary hydroxyl groups of the GPUs are oriented toward the narrow (tail) and wide (head) edges of the cone, respectively. There is no systematic variation of the physicochemical properties of native CDs with their number of GPUs. For instance, the solubilities of α -, β -, and γ -CDs are 149, 16.3, and 179 mM, respectively.¹ Because of the structural properties of native (and chemically modified) CDs that allow them to host hydrophobic molecules in its cavity giving rise to inclusion complexes, and due also to their low toxicity, a huge number of applications in different areas including paints, pharmacy, food, cosmetics, agrochemistry, analytical chemistry, catalysis, and chemosensor industries have been proposed.^{2–6} Interesting CD-based structures like nanotubes (or nanocolumns) have been characterized by different techniques such as NMR spectroscopy, X-ray diffraction, small-angle X-ray and neutron

scattering, scanning electron microscopy, (cryogenic) transmission electron microscopy, dynamic and static light scattering, atomic force microscopy, and computational calculations.^{7–13} It was shown that the structural and physicochemical features of those aggregates differ for each cyclodextrin. In particular, β -CD forms larger and more persistent aggregates than α -CD and γ -CD.

Native CDs do not exhibit a significant surface activity; that is, the dependence of the surface tension on CD concentration when they are dissolved in water is practically negligible. Taking advantage of this property, several research groups have used the adsorption curves of different amphiphilic molecules as a function of CD concentration to determine the equilibrium constants of the corresponding inclusion complexes.^{14–17} Using a combination of different experimental and theoretical techniques including dynamic and equilibrium surface tension measurements, atomic force and Brewster angle microscopies and molecular dynamics simulations, it has been recently demonstrated that the lack of surface activity of native α -CD is compatible with its spontaneous adsorption to the water/air interface.¹⁸ A film of specifically oriented α -CD-dimers forming parallel tubes has been proposed as the most probable structure of the adsorbed cyclodextrins. In each dimer, the truncated cone shaped structure usually employed to represent cyclodextrins would change to nanocylinder-like blocks where the two α -CDs are faced by the side with the secondary hydroxyl groups, being connected by a tight network of hydrogen bonds. The accessibility of such empty structures from both the air and the aqueous phases suggests a method to modify the properties of the interfacial film in a flexible way. For instance, it has been shown that the inclusion of the ionic surfactant sodium dodecyl

* To whom correspondence should be addressed. E-mail: angel.pineiro@usc.es.

[†] Universidad de Santiago de Compostela.

[‡] Universidad Nacional Autónoma de México.

[§] Current address: Computational Biochemistry and Biophysics Laboratory, Research Unit on Biomedical Informatics (GRIB)-IMIM/Universitat Pompeu Fabra, Parc de Recerca Biomèdica de Barcelona (PRBB), E-08003 Barcelona, Spain.

^{||} Current address: Department of Chemical Engineering, University of California, Santa Barbara, CA 93106, USA.

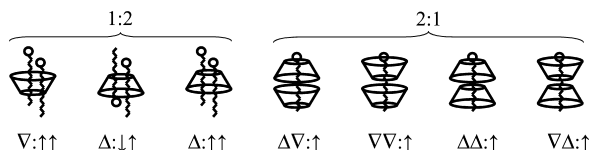


Figure 1. Schematic representation and symbol definitions employed throughout the text to refer to the starting conformations of the MD simulations.

sulfate (SDS) in such α -CD nanocylinders extensively modifies the mechanical properties of the film, as revealed by viscoelasticity and maximum drop volume measurements at low temperature and in a narrow range of relative concentrations of both solutes.^{18,19} It was also found that the structure and relative concentration of the chemical species in the bulk of the solution is crucial for the control of the interfacial film mechanical properties: the higher the relative amount of 2:1 α -CD₂SDS₁ complexes in the bulk phase, the higher the viscoelasticity of the corresponding surface film. For the sole native CDs, the adsorption constants to the solution/air interface have been estimated to be 10.7, 49.4, and 14.6 for α -, β -, and γ -CD, respectively,²⁰ in agreement with the significant lower solubility¹ of β -CD and its higher persistency to form aggregates.⁸ Then, although the above-mentioned comprehensive physicochemical study has been done only for the smallest native cyclodextrin, the fact that β - and γ -CDs were also found to adsorb to the solution/air interface indicates that, as with α -CD, these two cyclodextrins might form similar films at the solution/air interface. All of these findings open an avenue for the design of CD-based surface films with specific properties that could be controlled by changes of temperature and the addition of different cosolutes, encouraging us to characterize the potential films formed by β - and γ -CDs. Since it is expected that the species present in the interfacial phase are determined by those at the bulk, a first step toward those long-term goals is presented in this work, namely, a comprehensive structural–dynamic study of inclusion complexes formed by α -, β -, and γ -CDs with SDS at three temperatures, based on molecular dynamics (MD) computational simulations.

2. Methods: MD Simulations

2.1. Setup of the Simulation Boxes. The initial coordinates of α -CD, β -CD, γ -CD, and SDS molecules were taken from the Brookhaven Protein Data Bank²¹ (1BTC, 3CGT, 1D3C, and 1H0J codes, respectively). Since it is unlikely to observe the spontaneous formation of all possible inclusion complexes in the typical time scales reachable with MD simulations, we decided to start from seven different conformations for CD₁SDS₂ and CD₂SDS₁ complexes (Figure 1). To identify each of them throughout the text, the following notation is employed: Δ and ∇ represent a cyclodextrin with its narrow rim up and down, respectively, while \uparrow stands for one SDS molecule with the polar head up (down for \downarrow). Thus, the initial structures $V:\uparrow\uparrow$, $\Delta:\downarrow\uparrow$, and $\Delta:\uparrow\uparrow$ correspond to all possible relative orientations that CD and SDS molecules can adopt in inclusion complexes with a 1:2 stoichiometry, while the set composed of $\Delta\nabla:\uparrow$, $V\nabla:\uparrow$, $\Delta\Delta:\uparrow$, and $V\Delta:\uparrow$ represents all feasible 2:1 conformations. Periodic boundary conditions with a rhombic dodecahedron box as the basic unit cell were employed. The size of the simulation boxes was chosen such that the distance between the centers of two contiguous periodic images was 7 nm. Boxes were filled with ~8000 pre-equilibrated water molecules, and the system energy was minimized. To neutralize the charge of the system due to the ionic head of the surfactant, one sodium ion per SDS molecule was added.

2.2. Simulations Parameters. MD simulations were carried out using the GROMACS package^{22–24} (version 3.3.1) together with the simple point charge (SPC) water model²⁵ as explicit solvent and the 53a6 parametrization of the GROMOS96 force field^{26,27} for the cyclodextrins. This version of the GROMOS force field has specific parameters for saccharides, and hence it is expected to be reliable for the systems studied here. Parameters taken from the literature were employed for the SDS ionic head.²⁸ All of the simulations were performed in the *NPT* ensemble. Water, CD, SDS, and its counterion were coupled separately to an external temperature bath at 283, 298, or 323 K (using a coupling constant of 0.1 ps) by means of a Berendsen thermostat.²⁹ The pressure was maintained by weak coupling to 1 bar by means of a Berendsen barostat,²⁹ with a coupling time of 0.5 ps and an isothermal compressibility of 4.6×10^{-5} bar⁻¹. The initial velocities of the atoms were randomly assigned to produce a Maxwell distribution corresponding to the desired simulation temperature. The equations of motion were integrated using the leapfrog method with a 2 fs time step. The bond lengths and H–O–H angle in water were constrained using the SETTLE algorithm,³⁰ while the LINCS³¹ algorithm was used to constrain bond lengths in the SDS and CD molecules. Nonbonded interactions were evaluated using a twin range cutoff of 0.8 and 1.4 nm. Interactions within the shorter and longer cutoffs were updated every step and every five steps, respectively. Beyond the 1.4 nm cutoff a reaction field correction was performed with the same dielectric constant ($\epsilon = 62.0$) used to parametrize the force field. This approach for the long-range interactions was considered to be reasonable because all of the distances between atoms in the stable complexes are lower than the cutoff.

Each system was simulated for 10 ns, with configurations stored every 10 ps for analysis. It is worth mentioning that both dissociation and formation of cyclodextrin:surfactant complexes have been previously observed in this time scale.²⁰ Thus, it is expected that individual molecules of the unstable CD₁SDS₂ or CD₂SDS₁ conformations fell apart during the simulations to produce 1:1 species accompanied by a free surfactant or cyclodextrin molecule. In contrast, other initial conformations are expected to change their structure, optimizing the atomic interactions to furnish stable complexes. Eventually, the solutes might dissociate to give three free molecules in solution.

2.3. Analysis of the Trajectories. In total, 63 trajectories were generated corresponding to seven different initial conformations (Figure 1) at three temperatures for each of the three native α -, β -, and γ -cyclodextrins. The analysis of each of the 10 ns long MD trajectories was performed as follows. First, snapshots of the initial and final conformations of the complexes were created using PyMOL 0.99.³² In the cases where the complex is dissociated after 10 ns of simulation, the final state can be either a 1:1 complex plus one free molecule or three free molecules in solution or any intermediate arrangement. Distances between all pairs of molecules (except those of water) in each simulation box were calculated as a function of time, taking the respective centers of mass as positional references. The root-mean-square positional deviation (RMSD) of the cluster consisting of the three molecules was also calculated as a function of time regardless of whether or not they remain together, taking the corresponding initial conformation as the reference. The number of intramolecular hydrogen bonds in the CDs and the number of intermolecular H-bonds between CD and SDS were determined using a donor–acceptor cutoff distance of 0.35 nm and an angle donor–hydrogen acceptor smaller than 30°. The number of H-bonds established between

TABLE 1: Final Conformations for Native Cyclodextrins and SDS after 10 ns Trajectories^a

| initial conformation: | $\nabla:\uparrow\uparrow$ | $\Delta:\uparrow\uparrow$ | $\Delta:\uparrow\uparrow$ | $\Delta\nabla:\uparrow$ | $\nabla\nabla:\uparrow$ | $\Delta\Delta:\uparrow$ | $\nabla\Delta:\uparrow$ | |
|-----------------------|---------------------------|-----------------------------------|--|-----------------------------------|-------------------------|--------------------------|--------------------------|--------------------------|
| α -CD | 283 K | $\nabla:\uparrow\uparrow\uparrow$ | $\Delta:\uparrow\uparrow$ | $\Delta:\uparrow\uparrow\uparrow$ | $\Delta\nabla:\uparrow$ | $\nabla\nabla:\uparrow$ | $\Delta\Delta:\uparrow$ | $\nabla\Delta:\uparrow$ |
| | 298 K | $\nabla:\uparrow\uparrow\uparrow$ | $\Delta:\uparrow\uparrow$ | $\Delta:\uparrow\uparrow\uparrow$ | $\Delta\nabla:\uparrow$ | $\nabla\nabla:\uparrow$ | $\Delta\Delta:\uparrow$ | $\nabla\Delta:\uparrow$ |
| | 323 K | $\nabla:\uparrow\uparrow\uparrow$ | $\Delta:\uparrow\uparrow\downarrow$ | $\Delta:\uparrow\uparrow\uparrow$ | $\Delta\nabla:\uparrow$ | $\nabla+\nabla:\uparrow$ | $\Delta\Delta:\uparrow$ | $\nabla\Delta:\uparrow$ |
| β -CD | 283 K | $\nabla:\uparrow\uparrow\uparrow$ | $\Delta:\uparrow\downarrow$ | $\Delta:\uparrow\uparrow$ | $\Delta\nabla:\uparrow$ | $\nabla/\nabla:\uparrow$ | $\Delta\Delta:\uparrow$ | $\nabla\Delta:\uparrow$ |
| | 298 K | $\nabla:\uparrow\uparrow\uparrow$ | $\Delta:\uparrow\downarrow$ | $\Delta:\uparrow\uparrow$ | $\Delta\nabla:\uparrow$ | $\nabla+\nabla:\uparrow$ | $\Delta\Delta:\uparrow$ | $\nabla\Delta:\uparrow$ |
| | 323 K | $\nabla/\uparrow\uparrow\uparrow$ | $\Delta:\uparrow\downarrow$ | $\Delta:\uparrow\uparrow$ | $\Delta\nabla:\uparrow$ | $\nabla+\nabla:\uparrow$ | $\Delta\Delta:\uparrow$ | $\Delta+\nabla:\uparrow$ |
| γ -CD | 283 K | $\nabla:\uparrow\uparrow$ | $\Delta:\uparrow\downarrow/\downarrow$ | $\Delta:\uparrow\uparrow$ | $\Delta\nabla:\uparrow$ | $\nabla\nabla:\uparrow$ | $\Delta\Delta:\uparrow$ | $\nabla+\Delta:\uparrow$ |
| | 298 K | $\nabla:\uparrow\uparrow$ | $\Delta:\uparrow\downarrow$ | $\Delta:\uparrow\uparrow$ | $\Delta\nabla:\uparrow$ | $\nabla/\nabla:\uparrow$ | $\Delta+\Delta:\uparrow$ | $\Delta+\nabla:\uparrow$ |
| | 323 K | $\nabla:\uparrow\uparrow$ | $\Delta+\downarrow\uparrow\uparrow$ | $\Delta:\uparrow\uparrow$ | $\Delta\nabla:\uparrow$ | $\nabla\nabla:\uparrow$ | $\Delta\Delta:\uparrow$ | $\Delta+\nabla:\uparrow$ |

^a The + and/characters separating two species indicate lack of interaction and interaction giving rise to a noninclusion complex, respectively. Both characters shown simultaneously stand for borderline cases between a noninclusion complex and a noninteracting species.

the CD or SDS and any water molecule in the simulation box was estimated in the same way. These H-bond countings were performed throughout the 10 ns of each trajectory. Finally, the number of water molecules inside the cyclodextrins was calculated using spheres of diameter 0.90, 1.04, and 1.20 nm for α -, β -, and γ -CD, respectively, corresponding to the largest distance between two oxygen atoms linking the GPUs in the crystal structures of the CDs. At any time in the trajectory, these spheres were centered in the geometrical center of all of the oxygen atoms joining the glucopyranoside rings. Additionally, the number of water molecules located within the hydration shell (considered as 4 Å) of SDS was counted for some selected trajectories. Altogether, this analysis allows surveying quite clearly the time evolution of the preformed structures, including the moment at which any molecule falls apart from the cluster. It also made it possible to describe solute–solute and solute–solvent interactions. All figures and snapshots generated from this analysis are provided as Supporting Information (SI). We decided to restrict the present study to structural and dynamic properties because, in contrast to other properties like the density or the total energy of the system, they are highly sensitive to the formation and rupture of the complexes. On the other hand, as will be shown in the following sections, the analysis performed provides information useful to understand the main interactions between the molecules composing the supramolecular aggregates as well as their interaction with the solvent molecules. Free energy calculations for these systems are complicated for several reasons: (i) a complete thermodynamical characterization of the studied systems would require considering several hundred processes including the formation of 1:1, 2:1, and 1:2 stoichiometries with different relative orientations of the three molecules in the aggregates for three cyclodextrins at three temperatures and taking into account both inclusion and noninclusion complexes; (ii) the presence of three molecules in the aggregates introduces additional difficulties by increasing the complexity of the conformational space to be sampled as a function of any reaction coordinate and by affecting the definition of the initial and final states; and (iii) there are huge discrepancies in the reported ΔG° data for the formation of CD:SDS complexes [at least 37 different ΔG° values for β -CD₁SDS₁ complexes were found in the literature, ranging from 0.21 to 49 mM⁻¹ (unpublished data compilation)], and hence no reliable reference values are available.

3. Results and Discussion

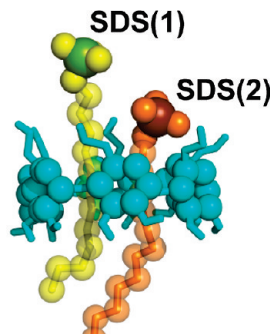
For a better understanding, this section and the SI should be read simultaneously.

3.1. Structural and Dynamic Characterization of CD:SDS Complexes. Similarities and Differences. MD simulations were performed for α -, β -, and γ -CDs with SDS in water at

283, 298, and 323 K. The aim was to provide fine structural–dynamic information about the inclusion complexes that can be formed by the native CDs and that anionic surfactant in aqueous solution. Table 1 provides a schematic overview of the final conformations encountered after 10 ns of MD simulation. The snapshots and plots resulting from the analysis of the 63 MD trajectories (performed as described in Section 2.3) are presented as SI. Here, only the most representative data are displayed (Figures 2–5). The MD results are presented separately for each CD and for each starting stoichiometry. To distinguish between the two identical molecules in 1:2 and 2:1 stoichiometries, the following notation is used all throughout this work, and the SI: SDS(1) stands for the SDS molecule whose head is further from the center of mass of the CD in any starting arrangement of the type 1:2, while CD(1) denotes the CD molecule that is closer to the SDS head in an initial 2:1 configuration. In the pictures, SDS(1) and CD(1) are colored yellow, whereas SDS(2) and CD(2) are shown in orange. For clarity, cyclodextrins are represented by a combination of spheres (atoms of the GPU rings) and sticks (primary and secondary hydroxyls).

Complexes Starting from α -CD₁SDS₂ Conformations. Among the three 1:2 complexes studied ($\nabla:\uparrow\uparrow$, $\Delta:\uparrow\uparrow$, and $\Delta:\uparrow\uparrow$), only those starting from the $\Delta:\uparrow\uparrow$ arrangement at 283 and 298 K were stable in the time scale of 10 ns. The SDS(1) fell apart from the later conformation at 323 K and from $\nabla:\uparrow\uparrow$ and $\Delta:\uparrow\uparrow$ at the three temperatures. The detachment of one SDS molecule can be explained by the repulsive interaction between the charges of the two ionic heads in the initial structure and by the limited dimensions of the α -CD cavity. The antiparallel relative orientation of the SDS molecules in the α -CD₁SDS₂ complexes that were observed to be stable during 10 ns favors the 1:2 stoichiometry. However, it can be seen in the distance plots that other α -CD₁SDS₂ complexes were stable for a significant part of the trajectories, namely: those starting from $\Delta:\uparrow\uparrow$ at 283 (Figure 2A) and 298 K were stable for 5 ns, the one starting from $\nabla:\uparrow\uparrow$ at 298 K kept its structure for 2 ns, and the same applies to the antiparallel arrangement ($\Delta:\uparrow\uparrow$) at 323 K. In the remaining structures the SDS(1) molecule left the cluster after a few picoseconds. Overall, most of the trajectories led to stable 1:1 complexes (Figure 2A). The number of hydrogen bonds between the α -CD and water molecules ranges from 22 to 30 for all of the trajectories, with a slight tendency to decrease with increasing temperature. SDS molecules that leave the complex set up about 8 simultaneous H-bonds with water molecules, while those remaining inside the cyclodextrin cavity may establish as few as 3. The number of H-bonds between the α -CD and the SDS polar head does not exceed 4 in all cases. Unsurprisingly, the number of SDS(i)–water and CD–SDS(i)

Starting Conformation

**A**

Final Conformation

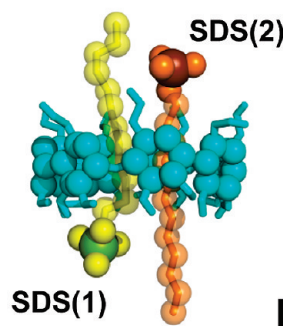
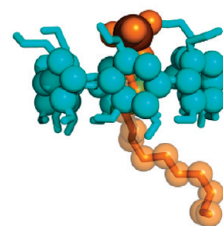
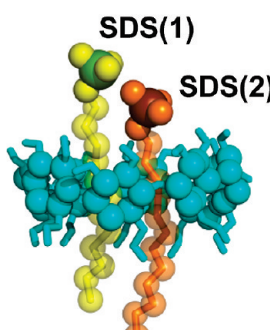
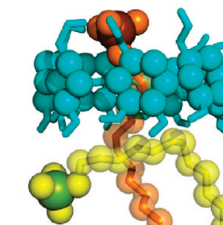
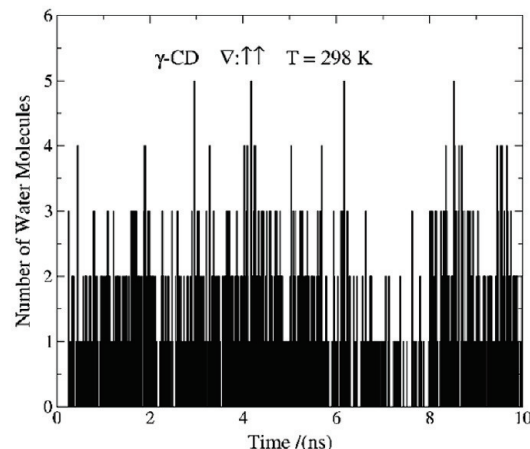
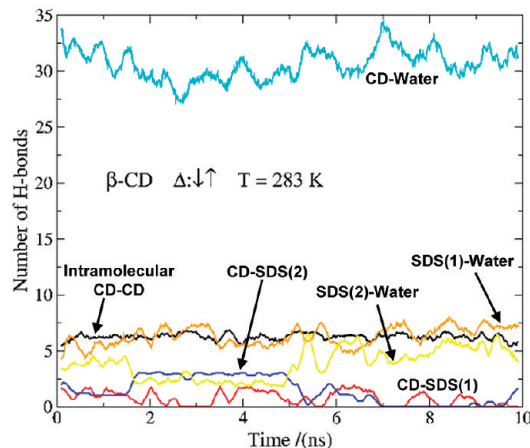
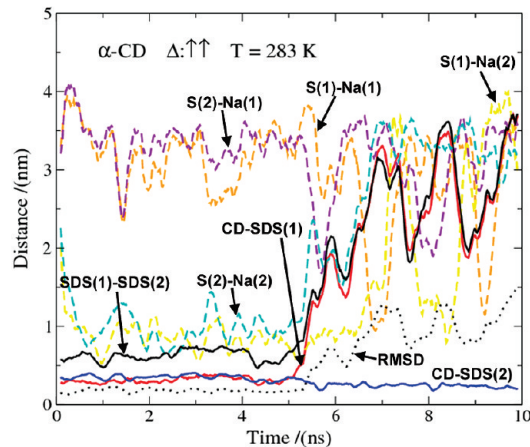
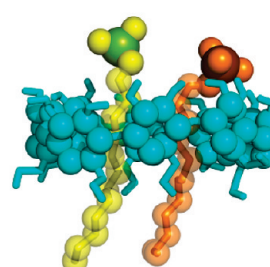
**B****C**

Figure 2. Representative results obtained by MD simulations starting from 1:2 complexes involving α - (A), β - (B), and γ -CD (C). The initial (left) and final (right) snapshots after 10 ns are shown for the conformations and temperatures indicated in the plots. Graph A represents the RMSD (black dotted) of the whole structure, and the intermolecular distances between CD-SDS(1) (red solid), CD-SDS(2) (blue solid), S(1)-Na(1) (orange dashed), S(1)-Na(2) (yellow dashed), S(2)-Na(1) (violet dashed), S(2)-Na(2) (cyan dashed), and SDS(1)-SDS(2) (black solid) as a function of time. Graph B represents the intramolecular hydrogen bonds of the cyclodextrin (black solid) and the intermolecular hydrogen bonds between CD-SDS(1) (red solid), CD-SDS(2) (blue solid), CD-H₂O (cyan solid), SDS(1)-H₂O (orange solid), and SDS(2)-H₂O (yellow solid) as a function of time. Graph C represents the number of water molecules inside of the cyclodextrin cavity as a function of time.

hydrogen bonds ($i = 1, 2$) correlate inversely with each other. On the other hand, the number of intramolecular H-bonds of the cyclodextrin is almost constant (~ 5), although it is reduced to ~ 3 for the two cases where both SDS molecules remain into the cavity. In such instances, two of the hydroxyl groups of the CD break the intramolecular H-bond connecting them to form

another one with the additional SDS molecule. The number of water molecules inside the α -CD is zero for all of the complexes at the three temperatures regardless of whether the stoichiometry of the final complex is 1:1 or 1:2. Only 1 marginal water molecule crosses the sphere identified as the cavity from time to time, with a higher frequency at 323 K.

Complexes Starting from α -CD₂SDS₁ Conformations. All of the structures were stable after 10 ns, except for that obtained from the $\nabla\nabla:\uparrow$ arrangement at 323 K, which led to a 1:1 complex when the CD(2) fell off after 4 ns. With this exception, all of the CD-CD and CD-SDS distances remained practically constant (an example is shown in Figure 3A). The final pictures show two clear trends. (i) For $\Delta\nabla:\uparrow$ and $\Delta\Delta:\uparrow$ complexes, both α -CDs are well-threaded by the SDS, in such a way that the ensemble looks like a [3]rotaxane (Figure 3A).³³ As with the 1:2 stoichiometry, the presence of water molecules inside any of the α -CDs is a scarce event along the trajectory. (ii) For the $\nabla\nabla:\uparrow$ and $\nabla\Delta:\uparrow$ configurations, even when the complex remains as such (five of six instances), only the very end of the SDS tail is inside the CD(2) cavity. Remarkably, the CD-CD and CD(2)-SDS distances are similar to each other and somewhat larger than their counterparts for the two other conformations, ranging from 0.8 to 1.0 nm. The α -CD(2) often hosts 1 to 2 water molecules in the trajectories starting from $\nabla\Delta:\uparrow$, and it exhibits a similar behavior (even with higher frequency) in the trajectories involving $\nabla\nabla:\uparrow$, hosting up to 4 water molecules during many frames (and even 10 at one frame) at 323 K. Since the latter counting corresponds to the α -CD that dissociated from the complex, it is useful as a reference to assess the maximum number of water molecules that one α -CD in aqueous solution is able to host in its cavity (as compared with the 5–6 waters found in the X-ray crystal structures, with two of them bonded to peripheral hydroxyl groups³⁴). The examination of the above-mentioned trends, together with the observation that the RMSD is more stable for the trajectories starting from $\Delta\nabla:\uparrow$ and $\Delta\Delta:\uparrow$, suggest that these configurations give rise to tighter α -CD₂SDS₁ complexes. The number of SDS-water H-bonds ranges from 2 to 6, attaining the lowest values for those tighter configurations and varying inversely with the number of CD(1)-SDS H-bonds. As expected, no hydrogen bond is observed between α -CD(2) and SDS. Except for the case of the trajectory that produced the 1:1 complex plus one free cyclodextrin, the number of H-bonds between CDs and water molecules is in average significantly lower than that obtained for the 1:2 stoichiometry. The obvious reason is that the hydroxyl groups of CDs are involved in CD-CD H-bonds. This is notable mainly in the case of the $\Delta\nabla:\uparrow$ arrangements, which exhibit an approximately constant value of 9 CD-CD H-bonds at 283 and 298 K (about 8 at 323 K), giving rise to nearly fixed CD-CD distances, in a structure where each CD molecule has switched from the cone shape to a cylindrical geometry (Figure 3A). Outstandingly, both CDs display 6 intramolecular H-bonds along these specific trajectories, whereas for the others it ranges from 2 to 5. As a result of such a special behavior, the number of CD-water H-bonds takes the lowest values (~17) in the trajectories starting from the $\Delta\nabla:\uparrow$ configurations. A similar trend had already been observed for complexes involving the nonionic surfactant octyl- β -D-glucopyranoside and displaying the same CD relative orientation.²⁰

Complexes Starting from β -CD₁SDS₂ Conformations. The results for β -CD are roughly similar to those involving α -CD. In most cases, one of the SDS molecules left the cavity giving rise to a 1:1 inclusion complex. Again, only two trajectories led to stable 1:2 complexes, namely, those starting from the $\Delta:\uparrow\uparrow$ arrangement at 283 and 298 K. The seemingly increased stability of this structure as compared with that built with α -CD probably arises from the larger diameter of the β -CD, which allows the coexistence of two anionic SDS-heads in the same side of its cavity. Notably, the final picture at 10 ns for five of nine trajectories shows a SDS molecule that is interacting with

the cyclodextrin after having left the cavity, lying perpendicularly to its main axis on one of the CD rims (Figure 2B). This kind of intermediate structure might not be classified as a 1:2 inclusion complex but proved to be very stable; in fact, that cluster arrangement was maintained from the beginning of the trajectory in two of those five instances. Moreover, in two other cases such an array was reached from the free state; that is, the SDS molecule fell apart from the complex very quickly, traveled all-around the simulation box for 5 and 7 ns ($\nabla:\uparrow\uparrow$ and $\Delta:\uparrow\uparrow$, respectively, at 323 K), and finally went to lie on the plane of the cavity, as if it felt attracted by the CD cavity. This suggests that SDS/ β -CD₁SDS₁ or SDS/ β -CD complexes could actually be formed and are not an artifact produced by the initial structure. Two arrays are possible, depending on whether the out-of-the-cavity SDS molecule is interacting with a free CD or with a 1:1 inclusion complex. The first case is exemplified by the snapshot at 10 ns and 323 K for the $\nabla:\uparrow\uparrow$ configuration, while the second one corresponds to the final pictures for $\Delta:\uparrow\uparrow$ at the three temperatures and for $\Delta:\uparrow\uparrow$ at 323 K (see SI). Similar arrays were found in simulations of β -CD with a nonionic surfactant.²⁰ It is worth noting that in these four examples of 1:2 intermediate arrangements the outer SDS is lying on the widest rim of the β -CD, while the inner SDS has its head oriented toward the narrowest rim. The hydrogen bond profiles for the simulations starting from β -CD₁SDS₂ complexes are quite similar to those observed with α -CD. The main difference is the number of CD-water hydrogen bonds that, due to the existence of an additional glucopyranoside group, are significantly higher, fluctuating between 27 and 33 in most cases (Figure 2B). Exceptionally, after having reached the free state the β -CD of the trajectory starting from $\nabla:\uparrow\uparrow$ at 323 K exhibits up to 40 H-bonds with water, while its number of intramolecular H-bonds attains minimum levels (~2). An unambiguous inverse correlation between the intramolecular H-bonds in the β -CD and its H-bonds with water can be also found in the trajectory starting from $\Delta:\uparrow\uparrow$ at 323 K. As expected, the number of intramolecular β -CD H-bonds reaches in general higher values than for α -CD molecules (7 against 5), due to the presence of the additional glucopyranoside ring. Moreover, contrary to the trend found in α -CD₁SDS₂ simulations, the highest values and the greatest stability of the number of intramolecular β -CD H-bonds are exhibited in trajectories where the 1:2 complex was stable. The number of SDS-water H-bonds ranges from 3 to 8 as in the case of α -CD, and for every SDS molecule, it varies inversely with the number of CD-SDS H-bonds. The latter can rise up to 3 or 2 for β -CD₁SDS₂ and SDS/ β -CD₁SDS₁ complexes, respectively. Hence, from the overall comparison between α -CD and β -CD simulations starting from 1:2 conformations, it appears that α -CD₁SDS₂ complexes are stabilized by CD-SDS hydrogen bonds, which are favored by the disruption of intramolecular α -CD H-bonds, whereas the stabilization of β -CD₁SDS₂ complexes is assisted by a higher number of intramolecular β -CD H-bonds that tightens the β -CD structure and outlines better the hydroxyl groups in the cavity rims. In contrast with the α -CD, the β -CD often hosts water molecules in the trajectories starting from 1:2 stoichiometry, their number not exceeding 1 for 1:2 inclusion complexes, ranging from 1 to 3 for SDS/ β -CD₁SDS₁, eventually rising up to 4–5 for 1:1 inclusion complexes or up to 6 for the SDS/ β -CD arrays, and taking still higher values when the β -CD is free (a maximum of 9 was found at 323 K). This reveals that the 1:2 and 1:1 inclusion complexes are more efficient than the corresponding SDS/ β -CD₁SDS₁ and SDS/ β -CD arrangements in expelling water molecules from the β -CD cavity.

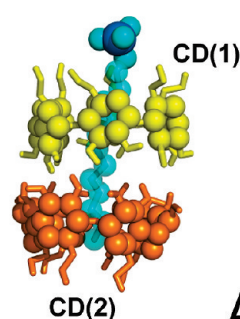
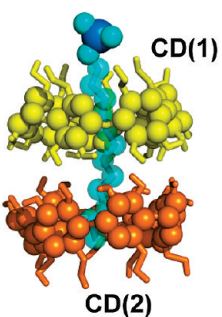
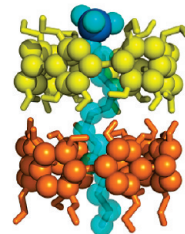
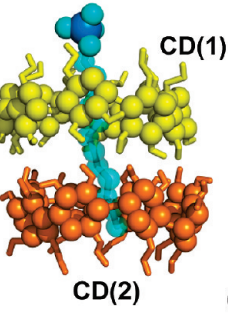
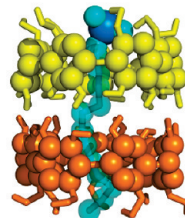
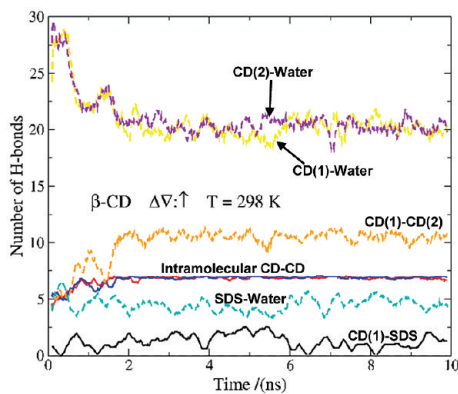
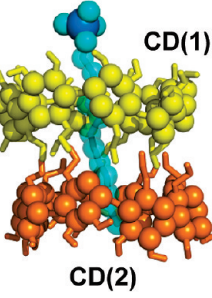
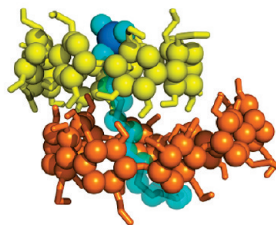
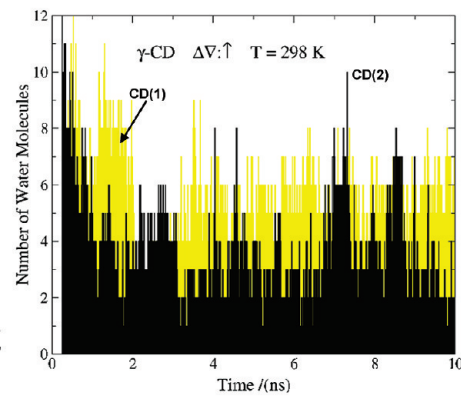
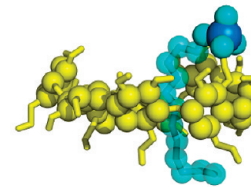
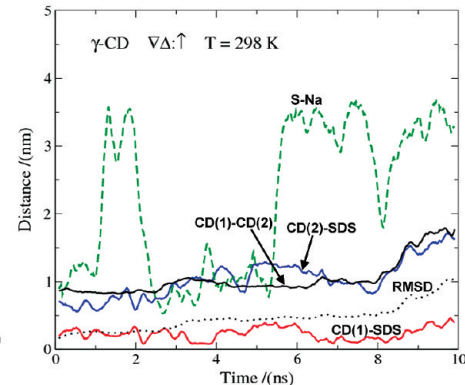
Starting Conformation**A****Final Conformation****B****C****D**

Figure 3. Representative results obtained by MD simulations starting from 2:1 complexes involving α - (A), β - (B), and γ -CD (C and D). The initial (left) and final (right) snapshots after 10 ns are shown for the conformations and temperatures indicated in the plots. The first and last graphs (A and D) represent the RMSD (black dotted) of the whole structure, and the intermolecular distances between CD(1)-SDS (red solid), CD(2)-SDS (blue solid), S-Na (green dashed), and CD(1)-CD(2) (black solid) as a function of time. Graph B represents the intramolecular hydrogen bonds of the CD(1) (red solid) and CD(2) (blue solid), and the intermolecular hydrogen bonds between CD(1)-CD(2) (orange dashed), CD(1)-H₂O (yellow dashed), CD(2)-H₂O (violet dashed), SDS-H₂O (cyan dashed), and CD(1)-SDS (black solid) as a function of time. Graph C represents the number of water molecules inside of the CD(1) (yellow) and CD(2) (black) cavities as a function of time.

Complexes Starting from β -CD₂SDS₁ Conformations. As with α -CD₂SDS₁ complexes, β -cyclodextrins seem to be stable as dimers threaded by one SDS molecule (Figure 3B). Except when starting from $\nabla\nabla:\uparrow$ at the three studied temperatures and from $\nabla\Delta:\uparrow$ at 323 K, all of the β -CD₂SDS₁ structures kept their original conformation in the time scale of 10 ns. Trajectories where the 2:1 arrangement was not stable led to the β -CD(2) molecule falling apart, producing a 1:1 complex. No significant changes are observed in the distances and RMSD curves for the trajectories where the 2:1 complexes preserved their structures. Moreover, the relative steadiness of the intermolecular distances during the simulations corresponding to $\Delta\nabla:\uparrow$ and, to a lesser extent to $\Delta\Delta:\uparrow$, suggests that these arrangements are significantly tighter than $\nabla\nabla:\uparrow$ and $\nabla\Delta:\uparrow$, as also found for α -CD₂SDS₁ conformations. The number of CD-water H-bonds varies from 20 per CD in the most stable configurations (Figure 3B) up to almost 40 for the β -CD(2) in those simulations where the 2:1 structure did not remain. As in the case of α -CD, the low number of CD-water H-bonds exhibited by the $\Delta\nabla:\uparrow$ arrangement at the three temperatures is ascribed to a relatively high degree of intermolecular and intramolecular CD-CD hydrogen bonding (\sim 11 and \sim 7, respectively, while they do not exceed 6 in any of the other trajectories). The H-bonds that the SDS establishes with water and with β -CD(1) correlate inversely, their amount being comparable to that found in the previously described configurations. As expected, no H-bonds are found between β -CD(2) and SDS in any of the analyzed trajectories. The β -CD(2) hosts typically from 1 to 4 water molecules in the stable 2:1 complexes regardless of the temperature, but after falling apart from the cluster such number fluctuates between 6 and 10 (although in one frame up to 12 water molecules were found inside the cavity). For comparison, 6 to 7 waters were found in X-ray crystal structures of free β -CD.³⁴ It is also observed that β -CD(1) rarely accepts more than 3 water molecules, even when becoming a part of a 1:1 complex. Overall, the analysis of the simulations starting from β -CD₂SDS₁ structures suggests that it is possible to find this stoichiometry and that, as in the case of α -CD, the $\Delta\nabla:\uparrow$ conformation should be very stable and tight (Figure 3B).

Complexes Starting from γ -CD₁SDS₂ Conformations. The simulations suggest that the 1:2 stoichiometry for γ -CD results in more stable complexes than for the two other CDs (Figure 2C). Thus, structures starting from $\nabla:\uparrow\uparrow$ and $\Delta:\uparrow\uparrow$ configurations were stable for the 10 ns at the three temperatures, while those starting from $\Delta:\downarrow\downarrow$ dissociated, leading to three free molecules in solution at 323 K and to a SDS/ γ -CD₁SDS₁ array at 283 and 298 K (the SDS(1) molecule left the CD cavity but kept interacting with its wider side). The intermolecular distances and RMSD reflect such a behavior since they do not exceed 0.5 and 0.3 nm, respectively, except for the simulations starting from $\Delta:\downarrow\downarrow$, for which the dissociated SDS(1) molecule remains at a distance of about 0.7 nm from the resulting 1:1 complex until the end of the trajectory (at 283 and 298 K) or for nearly 6 ns until the whole cluster breaks up (at 323 K). It is worth noting that the intermolecular distances for the stable γ -CD₁SDS₂ conformations exhibit larger fluctuations than those recorded for the stable α -CD₁SDS₂ and β -CD₁SDS₂ arrangements, accounting for the higher flexibility of the γ -CD. In the trajectories where the initial 1:2 configuration was held, the number of H-bonds between the γ -CD and water molecules approaches 35, decreasing slightly with temperature. That quantity rises to almost 40 for a poorly defined SDS/ γ -CD₁SDS₁ array (second half of the trajectory starting from $\Delta:\downarrow\downarrow$ at 283 K) and attains a value of 45 for free γ -CD ($\Delta:\downarrow\downarrow$ at 323 K, after 6

ns). Except for the latter, the number of CD-SDS hydrogen bonds (which rarely exceeds 3), the amount of those established between the SDS and water (3 to 8), and the number of intramolecular CD-CD H-bonds (\sim 7) are very similar in all of the trajectories. As with α -CD and β -CD, an inverse correlation between the number of CD-SDS(*i*) and SDS(*i*)-water hydrogen bonds is patent (*i* = 1, 2). Moreover, the number of intramolecular CD-CD H-bonds follows the trend already described for β -CD₁SDS₂ conformations, going down as the complex dissociates. The amount of water molecules hosted by the γ -cyclodextrin ranges typically from 1 to 3 in stable 1:2 complexes (Figure 2C), although a maximum of 5 water molecules seems to be compatible with this stoichiometry, and increases slightly with temperature. Some more water molecules (typically between 6 and 7) are observed inside the γ -CD in the case of a poorly defined SDS/ γ -CD₁SDS₁ array ($\Delta:\downarrow\downarrow$ at 283 K), while for simulation frames with free γ -CD that quantity rises up to 16.

Complexes Starting from γ -CD₂SDS₁ Conformations. Among the 12 MD simulations searching for γ -CD₂SDS₁ complexes, those starting from $\Delta\nabla:\uparrow$ at the three temperatures and from $\Delta\Delta:\uparrow$ and $\nabla\nabla:\uparrow$ at 283 and 323 K conserved the 2:1 stoichiometry after 10 ns of simulation (Figure 3C). For the trajectories starting from $\nabla\Delta:\uparrow$ at any temperature and from $\Delta\Delta:\uparrow$ and $\nabla\nabla:\uparrow$ at 298 K, the final array is a 1:1 complex (Figure 3D) plus one γ -CD that is either free or interacting laterally with the complex. The final γ -CD₂SDS₁ structures are in general much looser than the 2:1 complexes obtained with α - and β -CD. This feature is revealed by the distances and RMSD versus time plots, which allow describing the evolution of every complex structure throughout the trajectories. Thus, the intermolecular distances suffer significant fluctuations even for the most stable configurations, to such an extent that the CD(*i*)-SDS distance curves (*i* = 1, 2) approach closely or even intersect at many simulation times. This trend is unique to the γ -CD₂SDS₁ conformations. Moreover, these complexes can dissociate either by losing CD(1) or CD(2), since the SDS head may pass through the γ -CD(1) cavity. Such an occurrence, which was observed in two trajectories starting from $\Delta\Delta:\uparrow$ at 298 K and from $\nabla\Delta:\uparrow$ at 283 K, is unlikely with narrower cyclodextrins. Noticeably, CD(2)-SDS hydrogen bonds were detected at some instances in those trajectories. For γ -CD₂SDS₁ complexes, no significant differences are observed between the trajectories starting from $\Delta\nabla:\uparrow$ and from other initial conformations, in contrast with α -CD₂SDS₁ and β -CD₂SDS₁ conformations. The number of intramolecular CD-CD hydrogen bonds is even lower than that found for 2:1 complexes with α -CD and β -CD, despite the additional GPU present in γ -CD. The number of CD-water H-bonds varies typically from 30 to 40 as long as the γ -CD₂SDS₁ structure is kept, going up to 48 for free γ -CDs. All of these data indicate that the structural/dynamical behavior of the γ -CD is significantly different from that of α - and β -CD, due to its higher flexibility. The CD cavities host typically from 4 to 9 water molecules when the cyclodextrins are well-threaded with one SDS molecule (Figure 3C), but it increases to more than 15 for the free γ -cyclodextrins (21 was the maximum number recorded).

3.2. Contributions to the Formation of CD:SDS Inclusion Complexes.

The stabilization of CD-based inclusion complexes has been ascribed to five main contributions:³⁴ (i) the dehydration of the guest molecule chemical groups that are inserted into the CD cavity; (ii) the interaction of those groups with the interior of the cyclodextrin; (iii) the release of water molecules from the CD cavity to bulk water;³⁵ (iv) the conformational

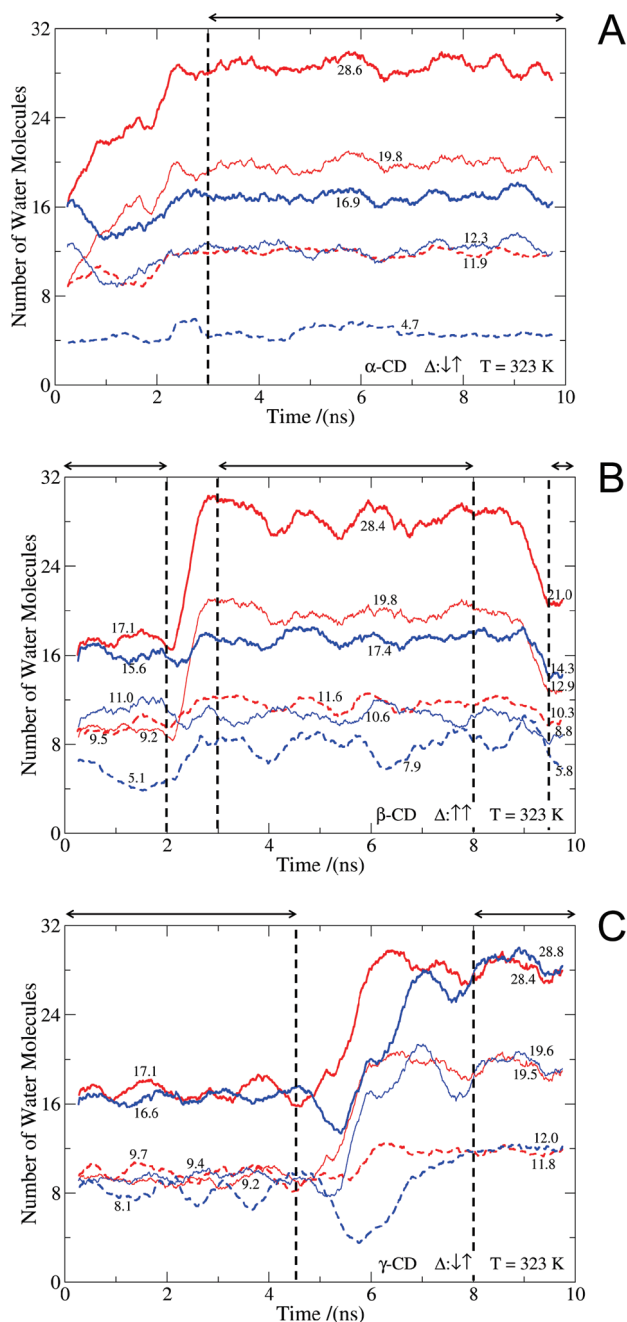


Figure 4. Number of water molecules located at less than 4 Å from any SDS atom (thick solid), from the oxygen or sulfur atoms in the SDS headgroup (dashed) and from the SDS tail carbon atoms (thin solid) as a function of time, for the trajectories corresponding to the 1:2 starting conformations and temperature indicated in the right bottom corner of each plot. The curves in red and blue represent the SDS(1) and SDS(2) surfactant molecules, respectively. Average values are specified next to each curve and correspond to the time range indicated by the arrows at the top of each plot and by the vertical dashed lines.

changes or strain release of the CD upon complexation; and (v) host–guest hydrogen bonding interactions. Some of these contributions have been discussed in detail in Section 3.1. In what follows, we present additional information provided by the MD simulations that pertain to them and also relate our findings with those in the literature.

In the specific case of SDS as a guest, the importance of the hydrophobic effect associated to contributions i–iii was revealed by Bo et al.,³⁶ who synthesized the $\beta\text{-CD}_1\text{SDS}_1$ species and

compared its ^1H NMR spectrum with that of the physical mixture of $\beta\text{-CD}$ and SDS, showing that the latter does not lead to inclusion, that is, that an aqueous solution is needed. As a general rule for surfactants, the first CH_2 group of the hydrophobic tail is expected to make little or no contribution to the hydrophobic effect, due to the partial charge induced by the proximity of the polar or ionic head.³⁷ However, alkyl sulfates (and in particular SDS) exhibit the opposite effect, since the oxygen atom linking the hydrocarbon chain to the sulfur atom of the sulfate group usually behaves as an extra methylene group.³⁷ This fact contributes to the stabilization of 2:1 species by allowing the SDS head to embed partially in the cavity of $\text{CD}(1)$, as seen in the final pictures of Figure 3A–C.

The hydration/dehydration of SDS molecules (contribution i) can be easily quantified from our trajectories. It is worth analyzing some cases (selected at the same temperature for comparison purposes) where at least one of the surfactant molecules departs from the cyclodextrin. For instance, SDS(1) separates from the initial $\Delta:\uparrow\uparrow$ complex with $\alpha\text{-CD}$ for the trajectory at 323 K, after nearly 2.5 ns (see SI). The difference between the number of water molecules in contact with both SDS molecules, one free and other threading the $\alpha\text{-CD}$ cavity, after that time measures the dehydration of SDS due to complexation. The average number of waters displaced from the surfactant anionic head, from the hydrocarbon tail, and from the whole molecule are 7.2, 7.5, and 11.7, respectively, as can be easily determined from Figure 4A. Note that the sum of the head and tail contributions does not match the value obtained for the whole SDS molecule because some waters are located simultaneously within the hydration shells (4 Å) of both SDS sections. It is interesting to observe the results of this calculation for the trajectory starting from $\Delta:\uparrow\uparrow$ with $\beta\text{-CD}$ at 323 K since one of the surfactant molecules leaves the complex at about 3 ns, moving around the simulation box for more than 5 ns, and going back to the 1:1 complex to form a noninclusion complex at about 9.5 ns (see Figure 4B and distances plot in the SI). From this trajectory it is possible to determine the head and tail contributions as well as the dehydration of the entire SDS molecule when forming a 1:1 and a noninclusion complex: (3.7, 9.2, and 11.0) and (1.3, 6.9, and 7.4) water molecules, respectively. It is noteworthy that the total number of water molecules in contact with the surfactant head in the 1:1 complex with $\beta\text{-CD}$ is significantly higher than that with $\alpha\text{-CD}$ at the same temperature (7.9 vs 4.7). This number decreases upon formation of the noninclusion arrangement $\beta\text{-CD}_1\text{SDS}_1/\text{SDS}$, reaching a value of 5.8. In fact, the formation of such a structure induces an extra dehydration of the SDS molecule that remains in the $\beta\text{-CD}$ cavity, releasing an average of 2.1, 1.8, and 3.1 water molecules from the head, the tail, and the total molecule, respectively. Since the presence of 1:2 complexes is expected to be significant in the case of $\gamma\text{-CD}$, it is convenient to determine the dehydration of SDS when forming such structures from the free species. The total rupture of a $\Delta:\uparrow\uparrow$ complex with $\gamma\text{-CD}$ takes place for the corresponding trajectory at 323 K. Both SDS molecules leave the CD cavity after 5–6 ns. According to Figure 4C, the changes in the number of water molecules located at less than 4 Å from the head, the tail, and the total molecule were (2.1, 10.3, and 11.3) and (3.9, 10.2, and 12.2) for SDS(1) and SDS(2), respectively. Again it is evident that the SDS-heads are more hydrated when the SDS threads a wider cavity. The trajectory with $\gamma\text{-CD}$ starting from $\nabla\Delta:\uparrow\uparrow$ at 323 K led eventually to a $\gamma\text{-CD}_1\text{SDS}_1$ complex, allowing the determination of the surfactant dehydration upon the formation of such 1:1 complex from the free SDS (third region

in Figure 4C): 3.2, 8.0, and 9.7 water molecules for the head and tail contributions, and for the whole molecule, respectively. The dehydration of the SDS tail upon 2:1 complex formation is expected to be significantly higher than the equivalent contribution for 1:1 species. Trajectories starting from $\Delta\nabla:\uparrow$ for α - and β -CDs, and from $\nabla\nabla:\uparrow$ for γ -CD, lead to stable 2:1 complexes at 323 K. The difference in the number of water molecules within the head, tail, and total-SDS hydration shells on going from those structures to the free SDS is (6.7, 15.5, and 19.5), (5.1, 16.2, and 19.2), and (3.3, 14.3, and 16.3) for α -, β -, and γ -CD, respectively. These data confirm the lower dehydration of the SDS head when increasing the number of cyclodextrin GPUs. They also reveal the higher dehydration of the SDS tail upon 2:1 complex formation with β -CD with respect to α -CD. This is due to the fact that β -CD enables the surfactant chain to coil by adopting *gauche* conformations, while the chain fraction included by α -CD adopts an all-*trans* conformation.³⁸

The MD simulations illustrate the importance of contribution iv, revealing the peculiar switch³⁹ from conical to cylindrical geometry suffered by the three cyclodextrins upon complexation. This can readily be seen comparing the snapshots at 0 and 10 ns for the configurations where at least a complex with 1:1 stoichiometry was stable in the studied time scale. This change in geometry was observed at the three studied temperatures, though for some 1:1 complexes where the SDS head approaches the entry of the CD cavity the conical shape seems to persist due to the attraction of the CD hydroxyl groups by the ionic head (see for example the final configuration of the trajectory starting from $\Delta:\uparrow\uparrow$ for β -CD at 298 K). The cone-to-cylinder geometrical change has already been observed in previous MD simulations of similar systems.^{18,20} An overview of all of the results from the MD simulations (Table 1) furnishes interesting additional information regarding contribution v. Both the H-bond analyses and the snapshots at 10 ns suggest that hydrogen bonding between the SO_4^- group and the CD hydroxyls contributes to the stability of the inclusion complexes. It is well-known that the values of the binding constants of surfactants with CDs depend, among other factors, on the formation of hydrogen bonds between the surfactant head groups and the hydroxyl groups located at the external surface of the CD cavity. This contribution depends on the nature of the headgroup of the surfactant.^{40–43} What is still a matter of controversy, at least in the case of SDS, is the inclusion mode. There is no agreement as to whether it is the primary (narrow edge or CD tail) or the secondary (wide edge or CD head) cyclodextrin hydroxyls that are nearer to the SDS-head. It is generally assumed that in the most likely mode of complexation, the polar group of the guest remains solvent exposed at the wide edge of the cavity.^{38,44,45} This assumption is supported by the fact that the CD tail was reported to be more lipophilic than the CD head.³⁸ However, Bo et al.^{36,46} concluded from ^1H NMR spectra that the SDS enters the β -CD cavity along its narrow rim, so that the SO_4^- group forms hydrogen bonds with primary hydroxyls. Their interpretation lay on the observation of a higher upfield shift of H-5 as compared to that of H-3 (inner protons^{47,48} located near the tail and head of β -CD, respectively). Puzzlingly, the same behavior (in ^1H NMR studies involving other surfactants) did not prevent other authors⁴⁸ from arriving to the opposite interpretation, namely, that the polar headgroup of the guest was located close to the wide edge of the β -CD. This disagreement reveals the difficulty of analyzing ^1H NMR data due to numerous antagonistic shielding and deshielding effects, as thoroughly explained by Wilson and Verrall.³⁸ Our MD

analysis shows: (a) starting from the $\Delta:\uparrow\uparrow$ arrangement, SDS(1) is more likely to fall apart from the complex than SDS(2); (b) $\Delta:\uparrow\uparrow$ conformations are more stable than $\nabla:\uparrow\uparrow$ ones; and (c) the $\Delta\nabla:\uparrow$ and $\Delta\Delta:\uparrow$ configurations exhibit a greater stability than $\nabla\Delta:\uparrow$ and $\nabla\nabla:\uparrow$. All of these findings support the conclusion reached by Bo et al. for β -CD:SDS species. In general, our results indicate that in most cases the SDS enters the CD cavity along its narrow edge to form 1:1 inclusion complexes, which are in part stabilized by H-bonding between the SO_4^- group and the primary hydroxyls of the corresponding CD. This preference may be related to the directionality of the dipole moment borne by the macrocycle, which is collinear to its longitudinal axis and points from the CD head to the CD tail.⁴⁹

3.3. CD Dimer as a Basic Building Block. Maximum drop volumes of α -CD + SDS aqueous solutions notably larger (up to $\sim 25\%$) than those of pure water were found at low temperatures and $[\alpha\text{-CD}]/[\text{SDS}]$ concentration ratios above 2.3.¹⁹ Relying on the high dependence on temperature of the equilibrium constant for the formation of the 2:1 complexes,¹⁸ that finding was ascribed to the high viscoelasticity of the solution/air interfacial film caused by the presence of the α -CD₂SDS₁ species. As regards β -CD₂SDS₁ complexes, they were reported to exhibit lower solubility than the β -CD₁SDS₁ species due to the intermolecular CD–CD hydrogen bonding, also suggesting a high affinity of 2:1 complexes for the interface.⁵⁰ Funasaki et al.⁵¹ concluded from rotating frame Overhause effect spectroscopy (ROESY) and ^1H NMR spectra that two α -CD molecules adopt mainly the $\Delta\nabla$ configuration when they shuttle on a dodecyl chain (dodecyltrimethylammonium bromide) to give the $\Delta\nabla:\uparrow$ complex. Previously, applying identical techniques to sodium dodecyl carboxylate complexes with α - and β -CD, Wilson and Verrall³⁸ had inferred that the four possible configurations for the 2:1 species ($\Delta\nabla:\uparrow$, $\nabla\nabla:\uparrow$, $\Delta\Delta:\uparrow$, and $\nabla\Delta:\uparrow$) occur in a random fashion. Among the 2:1 conformations studied here by MD simulation, those denoted as $\Delta\nabla:\uparrow$ for α - and β -CDs exhibit the highest number of intermolecular CD–CD H-bonds accompanied with a very tight structure. In this respect, it should be noted that the strong cooperativity observed in (α -CD)-based molecular necklaces threaded by polyethylene oxide chains (PEO) was ascribed to a high number of intermolecular H-bonds.⁵² The structure of CD:PEO complexes and also of CD aggregates were later studied by X-ray diffraction of precipitates.^{9,12} In general, columnar crystalline structures with an identical hexagonal arrangement of CDs in the basal plane but different periodicity along the columns were observed. The CD dimer in the $\Delta\nabla$ form was identified as the basic unit of crystals for α - and β -CD. Additionally, the alternative $\Delta\Delta$ arrangement was observed for α -CD. The crystals obtained from γ -CD exhibited a triple periodicity in the dimension of the columns based on head-to-head ($\Delta\nabla$), tail-to-tail ($\nabla\Delta$), and tail-to-head ($\nabla\nabla$) units. The MD results provided in this work show the dynamic behavior in solution of all of these conformations threaded by SDS. The MD trajectories strongly indicate that the most stable 2:1 complexes are those with the $\Delta\nabla:\uparrow$ conformation, signaling the different interactions that contribute to its stability. The $\Delta\nabla$ CD dimer was proposed as the building block for the nanotubular assemblies observed at the solution/air interface of α -CD + water and α -CD + SDS aqueous mixtures.¹⁸ Assuming that the structures present at the interface are determined by their presence in the bulk, there is clear evidence indicating that similar films could also be formed with β - and to a lesser extent with γ -CD. In particular, the low solubility,¹ high adsorption at the solution/air interface,²⁰ and great persistency in the formation

of aggregates⁸ of β -CD indicate that this macromolecule is promising for the design of functional CD-based films. In summary, it appears that the CD dimer is a basic building block for the formation of a variety of structures such as inclusion complexes, threaded molecular necklaces, columnar aggregates, and nanotubes at the liquid/air interface.

3.4. Noninclusion CD:SDS Complexes. The important contribution of noninclusion-based phenomena to drug solubilization by cyclodextrins was recently recognized and reviewed by Loftsson et al.,⁵³ motivating Alvira to analyze by MD simulations the mobility of rigid nonpolar linear molecules inside and around β -CD as a function of temperature, length of the guest, and Lennard-Jones potential parameters.⁵⁴ A reliable configuration for (β -CD)-based noninclusion complexes is shown in Figure 2B. The MD simulations also point to the presence of “intermediate arrangements” with γ -CD (see in the SI the results for the trajectory involving γ -CD at 298 K that starts from $\Delta:\ddagger$). These noninclusion complexes seem to be stable regardless of the temperature (at least for β -CD) and are also characterized by the fact that fewer water molecules are displaced from the CD cavity due to the presence of the second SDS molecule, whose hydrophobic tail remains partially solvated (see Section 3.2). SDS/CD₁SDS₁ (and SDS/CD) arrays have not been identified by experimental techniques that are highly sensitive to changes in the solvent-exposed hydrophobic area, like isothermal titration calorimetry, probably because they have not been explicitly considered in the employed models. Such arrays, which had already been observed in MD simulations of β -CD with the nonionic surfactant octyl- β -D-glucopyranoside,²⁰ might be conceived as intermediate structures in a mechanism where inclusion proceeds in two steps that cannot be clearly separated.⁵⁵ The two-stage inclusion process was suggested by Komiyama and Bender⁵⁶ for the inclusion of the relatively bulky 1-adamantanecarboxylate into β -CD. They concluded that the first stage (the guest sitting on top of the cavity) would be associated to quite favorable ΔS° and small favorable ΔH° , while the second step (accommodation of the guest within the cavity) would be accompanied by a large unfavorable ΔS° and a large favorable ΔH° . Hersey et al.³⁹ used kinetic methods to characterize that kind of intermediate species in the context of binding of azo-dyes to α -CD, finding that they are formed in a fast pre-equilibrium step, followed by a slower insertion of the guest into the host. This mechanism pertains to the case of classical competitive inhibition, such as those encountered in many enzyme systems.³⁹ On the other hand, on the basis of MD simulations performed for γ -CD in the presence of a SDS excess (not shown), we hypothesize that the SDS/CD₁SDS₁ and SDS/CD arrays could act as nucleation points for the reported (β -CD)-induced aggregation of SDS *below* its cmc.^{57–59} This is consistent with the idea, proposed by Jiang and Wang,⁵⁷ that the β -CD₁SDS₁ inclusion complex acts as the hydrophobic source inducing the SDS aggregation.

3.5. Role of the Na⁺ Counterions. The charge of the guest should destabilize some of the complexes with 1:2 stoichiometry, that is, some of the CD₁SDS₂ conformations, while the relatively large hydrophobic chain should partially compensate this effect and contribute to the stabilization of those structures as well as to the formation of CD₂SDS₁ arrays. Unexpectedly, as described in Section 3.1, at least one SDS molecule fell apart from the $\Delta:\ddagger$ configurations involving γ -CD at the three temperatures, while the 1:2 complexes were stable during the 10 ns trajectories when starting from $\nabla:\ddagger$ or $\Delta:\ddagger$, regardless of the temperature. This indicates that γ -CD₁SDS₂ species with a parallel orientation of SDS molecules are more stable than the corresponding

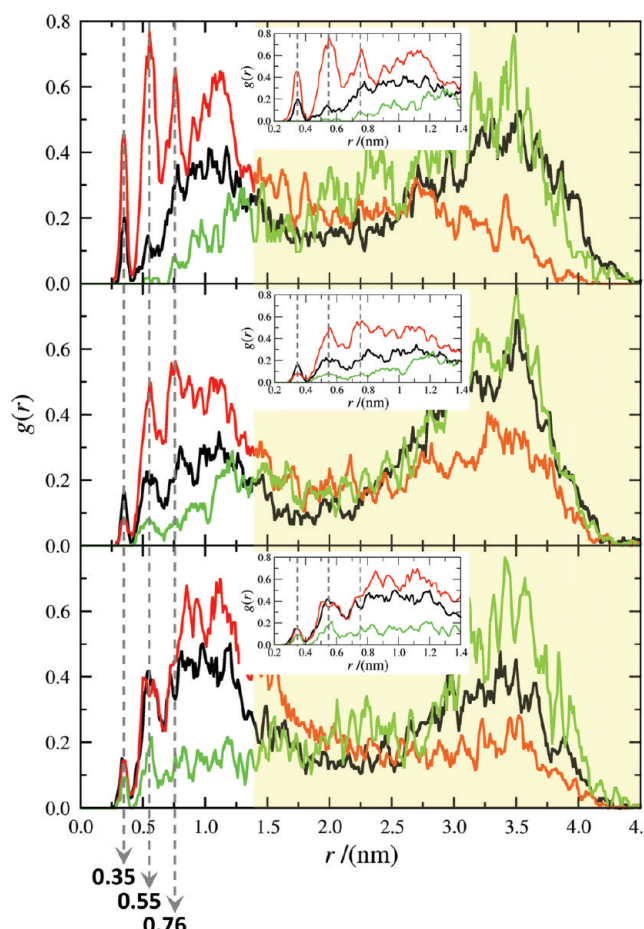


Figure 5. Radial distribution functions of SDS sulfur atoms to Na^+ counterions for the $\Delta:\ddagger$ (red), $\nabla:\ddagger$ (black), and $\Delta:\ddagger$ (green) γ -CD₁SDS₂ complexes at 283 K (top), 298 K (middle), and 323 K (bottom). Only the time intervals corresponding to stable complexes were considered for the $\Delta:\ddagger$ trajectories ([0, 3.10] ns for 283 K, [0, 9.40] ns for 298 K, and [0, 4.85] ns for 323 K), whereas the stability of the $\Delta:\ddagger$ and $\nabla:\ddagger$ conformations allowed us to employ the whole 10 ns. All $g(r)$ functions have been normalized so that the area under $g(r)$ is scaled to unity. The yellow shaded regions correspond to the r values beyond the cutoff used for the evaluation of the electrostatic interactions. The $g(r)$ values within the cutoff are expanded in the insets. The first three peaks at 0.35, 0.55, and 0.76 nm are marked with vertical gray dashed lines in both the main plots and the insets.

antiparallel conformation, which is paradoxical since one would expect the electrostatic repulsion between the anionic heads of parallel surfactants to be a source of instability. A rationalization for this finding can be found in the role played by the Na^+ counterions, whose trajectories were monitored in terms of the distances to the anionic SDS-heads (see distance plots in the SI, where S and Na stand for the headgroup sulfur atom and the sodium counterion, respectively). It is widely accepted that inorganic ions do not interact appreciably with CDs alone,⁴¹ but this agreement is not extended to their interaction with ionic encapsulated surfactants. Some authors assume, either implicitly^{42,60} or explicitly,⁶¹ that counterions do not bind to surfactant ions in the inclusion complex, while others even support such a statement with experimental evidence.⁶² However, the existence of counterion binding by β -CD:SDS complexes has been proved through selective ion electrode studies, where it was concluded that the Na^+ ion loses some mobility as a consequence of being held electrostatically by the CD included surfactant anion.⁶³ Even though in this work the long-range interactions were not explicitly considered beyond a 1.4 nm

cutoff, the Na^+ ions were seen to eventually approach the SDS ionic head close enough to be captured by electrostatic attraction in most of the trajectories (the first, second, and third binding shells have radii of 0.425, 0.675, and 0.925 nm, respectively, as measured from the sulfur atom by Sammalkorpi et al.⁶⁴). Nevertheless, the degree of counterion binding in 1:1 and 2:1 complexes was negligible regardless of the temperature or the CD size. In contrast, the 1:2 complexes arranged in parallel orientation and particularly those with the $\Delta:\uparrow\uparrow$ configuration involving γ -CD demanded the presence of at least one Na^+ ion to screen the electrostatic repulsion between the two SDS heads. This finding is illustrated by Figure 5, which shows the sulfur–sodium radial distribution function $g(r)$ for the three γ -CD₁SDS₂ conformations at each working temperature. The positions of the Na^+ ion condensation peaks for the first three binding shells were found at about 0.35, 0.55, and 0.76 nm, in good agreement with the reported values⁶⁴ (0.38, 0.58, and 0.78 nm). It becomes clear from Figure 5 that the counterion binding is privileged in the 1:2 conformations exhibiting parallel orientation of SDS molecules, with a prevalent occurrence in the case of $\Delta:\uparrow\uparrow$ at low temperatures. Moreover, according to Sammalkorpi et al.,⁶⁵ if the same Na^+ ion resides within a distance of 0.72 nm from two nearest-neighbor SDS head groups, a salt bridge is formed between these groups, its average lifetime being 80 ps at 323 K. In the present work, Na^+ mediated salt bridges obeying to that description were observed over significant fractions of the trajectories corresponding to the stable parallel 1:2 species ($\Delta:\uparrow\uparrow$ and $\nabla:\uparrow\uparrow$ for γ -CD at the three temperatures, and $\Delta:\uparrow\uparrow$ for β -CD at 283 and 298 K). More precisely, the percentage of bound counterions (through the first and second binding shells) taking part in Na^+ mediated salt bridges amounted to 18–38% for $\nabla:\uparrow\uparrow$ and 31–53% for $\Delta:\uparrow\uparrow$.

4. Conclusions

An extensive characterization of the structural and dynamic behavior of CD:SDS inclusion complexes involving α -, β -, and γ -CD by molecular dynamics simulations at 283, 298, and 323 K has been presented. These three temperatures were considered because previous experiments showed that the mechanical properties of α -CD:SDS complexes self-assembled films change sharply from 283 to 323 K.^{18,19} The MD results indicate that complexes with the $\Delta\nabla:\uparrow$ configuration are very tight due to a network of CD–CD H-bonds for α - and β -CD. These structures are also predicted to exist in the presence of γ -CD though they are much looser. The existence of tight $\Delta\nabla:\uparrow$ structures based on the three cyclodextrins is important because they have been proposed as the building blocks for the above-mentioned solution/air interfacial CD-based films, as well as for aggregates in the bulk phase. In particular, structures based on β -CD are promising for further studies because of the higher adsorption constant and lower solubility of this cyclodextrin together with its proved ability to self-aggregate in persistent nanotubular structures, which take place at a significantly lesser extent with α - and γ -CD.^{8,12} In addition to the 2:1 complexes based on γ -CD, the γ -CD₁SDS₁ and γ -CD₁SDS₂ species seem to coexist in the presence of this cyclodextrin. The simulations also suggested the existence of intermediate arrangements between 1:1 and 1:2 inclusion complexes, in which a SDS molecule is threading a β -cyclodextrin by pointing its head toward the narrow side of the CD cavity while a second SDS is lying on the plane of its wide side. Such noninclusion complexes were also observed for the simulations involving γ -CD, though not for α -CD, and it is suggested here that they could be the seed for premicellar surfactant aggregates in the presence of cyclo-

dextrins. The role of Na^+ counterions showed to be relevant to screen the electrostatic repulsion of the SDS heads in the $\Delta:\uparrow\uparrow$ and $\nabla:\uparrow\uparrow$ complexes involving γ -CD, since all of them were unexpectedly stable, exhibiting a significative degree of counterion binding and even the occurrence of Na^+ mediated salt bridges between the SDS head groups. Still, the counterions do not bind noticeably to the anionic SDS head in the 1:1 or 2:1 complexes, nor in the 1:2 complexes with antiparallel relative orientation of the SDS molecules. MD simulations confirmed and characterized the previously reported^{20,39} cone-to-cylinder CD conformational change accompanying the inclusion of a ligand. They also confirmed the lipophilic-like behavior of the oxygen atom linking the hydrocarbon chain to the sulfur atom in the SDS sulfate group; this group appears to be partially embedded in the cavity of CD(1) in CD₂SDS₁ complexes, playing the role of an extra methylene group. Furthermore, the preferred inclusion mode of SDS in native cyclodextrins seems to be entering the CD cavity along its narrow edge, the resulting 1:1 species being stabilized by hydrogen bonding between the SO_4^- group and primary hydroxyls of the CD. Overall, this work provides insight into the characterization of supramolecular complexes of cyclodextrins with SDS molecules at a high level of detail. It is hoped that our findings prove to be useful for the development of new materials with interesting specific properties. Further work needs to be performed to achieve a comprehensive thermodynamic and energetic characterization of these systems.

Acknowledgment. This work was supported by Grants J49811 and 99844 from CONACyT-México, Grants IN105107 and IN104210 from PAPIIT-DGAPA-UNAM, FIS2007-63479 from MEC-Spain, and INCITE08PXIB206050PR from XUGA-Spain. P.B. thanks the program “Recursos Humanos” of INCITE2007 from “Xunta de Galicia” for supporting her with a research stay grant. N.D.-V. is grateful for financial support from CONACyT. Á.P. thanks “Xunta de Galicia” for his “Isidro Parga Pondal” research position. We are grateful to the “Dirección General de Cómputo Académico” (DGSCA) of Universidad Nacional Autónoma de México (UNAM) and to the “Centro de Supercomputación de Galicia” (CESGA) for computing time and for their excellent services.

Supporting Information Available: Graphical analysis of the MD simulations distributed in four files containing, for each of the 63 trajectories: (i) snapshots of the initial and final conformations, (ii) RMSD of the complex and intermolecular distances along the trajectory, (iii) the number of intramolecular (for the CDs) and intermolecular H-bonds as a function of time, and (iv) the number of water molecules hosted by the cyclodextrins also as a function of time. Every file has seven pages, one for each of the conformations defined in Figure 1, where it is possible to compare the results for a given cyclodextrin at the three temperatures or between the three cyclodextrins at a given temperature. The organization of the four files is identical to facilitate the comparison of the different analysis performed for a given trajectory. This material is available free of charge via the Internet at <http://pubs.acs.org>.

References and Notes

- (1) Szejtli, J. Introduction and General Overview of Cyclodextrin Chemistry. *Chem. Rev.* **1998**, *98*, 1743–1754.
- (2) Buschmann, H.; Schollmeyer, E. Applications of Cyclodextrins in Cosmetic Products: A Review. *J. Cosmet. Sci.* **2002**, *53*, 185–191.
- (3) Del Valle, E. M. M. Cyclodextrins and their Uses: A Review. *Process Biochem.* **2004**, *39*, 1033–1046.

- (4) Challa, R.; Ahuja, A.; Ali, J.; Khar, R. K. Cyclodextrins in Drug Delivery: An Updated Review. *AAPS PharmSciTech* **2005**, *6*, E329–E357.
- (5) Loethen, S.; Kim, J.; Thompson, D. H. Biomedical Applications of Cyclodextrin-Based Polyrotaxanes. *Polym. Rev.* **2007**, *47*, 383–418.
- (6) Numanoglu, U.; Sen, T.; Tarimci, N.; Kartal, M.; Koo, O. M. Y.; Önyüksel, H. Use of Cyclodextrins as a Cosmetic Delivery System for Fragrance Materials: Linalool and Benzyl Acetate. *AAPS PharmSciTech* **2007**, *8*, 34–42.
- (7) Polarz, S.; Smarsly, B.; Bronstein, L.; Antonietti, M. From Cyclodextrin Assemblies to Porous Materials by Silica Templatting. *Angew. Chem., Int. Ed.* **2001**, *40*, 4417–4421.
- (8) González-Gaitano, G.; Rodríguez, P.; Isasi, J. R.; Fuentes, M.; Tardajos, G.; Sánchez, M. The Aggregation of Cyclodextrins as Studied by Photon Correlation Spectroscopy. *J. Inclusion Phenom. Macrocyclic Chem.* **2002**, *44*, 101–105.
- (9) Topchieva, I. N.; Tonelli, A. E.; Panova, I. G.; Matuchina, E. V.; Kalashnikov, F. A.; Gerasimov, V. I.; Rusa, C. C.; Rusa, M.; Hunt, M. A. Two-Phase Channel Structures Based on α -Cyclodextrin - Polyethylene Glycol Inclusion Complexes. *Langmuir* **2004**, *20*, 9036–9043.
- (10) Bonini, M.; Rossi, S.; Karlsson, G.; Almgren, M.; Lo Nstro, P.; Baglioni, P. Self-Assembly of β -Cyclodextrin in Water. Part 1: Cryo-TEM and Dynamic and Static Light Scattering. *Langmuir* **2006**, *22*, 1478–1484.
- (11) Topchieva, I. N.; Spiridonov, V. V.; Kalashnikov, P. A.; Kurganov, B. I. The Detection of Cyclodextrin Self-Association by Titration with Dyes. *Colloid J.* **2006**, *68*, 98–105.
- (12) Panova, I. G.; Matukhina, E. V.; Gerasimov, V. I.; Topchieva, I. N. Non-Covalent Columnar Cyclodextrin-Based Structures. *Colloid J.* **2006**, *68*, 66–78.
- (13) Topchieva, I. N.; Panova, I. G.; Kurganov, B. I.; Spiridonov, V. V.; Matukhina, E. V.; Filippov, S. K.; Lezov, A. V. Noncovalent Columnar Structures Based on β -Cyclodextrin. *Colloid J.* **2008**, *70*, 356–365.
- (14) Dharmawardana, U. R.; Christian, S. D.; Tucker, E. E.; Taylor, R. W.; Scamehorn, J. F. A Surface Tension Method for Determining Binding Constants for Cyclodextrin Inclusion Complexes of Ionic Surfactants. *Langmuir* **1993**, *9*, 2258–2263.
- (15) Funasaki, N.; Yodo, H.; Hada, S.; Neya, S. Stoichiometries and Equilibrium-Constants of Cyclodextrin-Surfactant Complexations. *Bull. Chem. Soc. Jpn.* **1992**, *65*, 1323–1330.
- (16) Funasaki, N.; Ohigashi, M.; Hada, S.; Neya, S. Surface Tensiometric Study of Multiple Complexation and Hemolysis by Mixed Surfactants and Cyclodextrins. *Langmuir* **2000**, *16*, 383–388.
- (17) Angelova, A.; Ringard-Lefebvre, C.; Baszkin, A. Drug-Cyclodextrin Association Constants Determined by Surface Tension and Surface Pressure Measurements: II. Sequestration of Water Insoluble Drugs from the Air-Water Interface: Retinol- β Cyclodextrin System. *J. Colloid Interface Sci.* **1999**, *212*, 280–285.
- (18) Hernández-Pascacio, J.; Garza, C.; Banquy, X.; Díaz-Vergara, N.; Amigo, A.; Ramos, S.; Castillo, R.; Costas, M.; Piñeiro, Á. Cyclodextrin-Based Self-Assembled Nanotubes at the Water/Air Interface. *J. Phys. Chem. B* **2007**, *111*, 12625–12630.
- (19) Hernández-Pascacio, J.; Banquy, X.; Pérez-Casas, S.; Costas, M.; Amigo, A.; Piñeiro, Á. A Small Molecular Size System Giving Unexpected Surface Effects: α -Cyclodextrin + Sodium Dodecyl Sulfate in Water. *J. Colloid Interface Sci.* **2008**, *328*, 391–395.
- (20) Piñeiro, Á.; Banquy, X.; Pérez-Casas, S.; Tovar, E.; García, A.; Villa, A.; Amigo, A.; Mark, A. E.; Costas, M. On the Characterization of Host-Guest Complexes: Surface Tension, Calorimetry, and Molecular Dynamics of Cyclodextrins with a Non-Ionic Surfactant. *J. Phys. Chem. B* **2007**, *111*, 4383–4392.
- (21) <http://www.pdb.org>.
- (22) Berendsen, H. J. C.; van der Spoel, D.; van Drunen, R. GROMACS: A Message-Passing Parallel Molecular Dynamics Implementation. *Comput. Phys. Commun.* **1995**, *91*, 43–56.
- (23) Lindahl, E.; Hess, B.; van der Spoel, D. GROMACS 3.0: A Package for Molecular Simulation and Trajectory Analysis. *J. Mol. Model.* **2001**, *7*, 306–317.
- (24) <http://www.gromacs.org>.
- (25) Berendsen, H. J. C.; Postma, J. P. M.; van Gunsteren, W. F.; Hermans, J. Interaction models for water in relation to protein hydration. In *Intermolecular Forces*; Pullman, B., Ed.; D. Reidel: Dordrecht, 1981; pp 331–342.
- (26) Schuler, L. D.; van Gunsteren, W. F. On the Choice of Dihedral Angle Potential Energy Functions for n-Alkanes. *Mol. Simul.* **2000**, *25*, 301–319.
- (27) Oostenbrink, C.; Villa, A.; Mark, A. E.; van Gunsteren, W. A Biomolecular Force Field Based on the Free Enthalpy of Hydration and Solvation: The GROMOS Force-Field Parameter Sets 53A5 and 53A6. *J. Comput. Chem.* **2004**, *25*, 1656–1676.
- (28) Schweighofer, K. J.; Essmann, U.; Berkowitz, M. Simulation of Sodium Dodecyl Sulfate at the Water-Vapor and Water-Carbon Tetrachloride Interfaces at Low Surface Coverage. *J. Phys. Chem. B* **1997**, *101*, 3793–3799.
- (29) Berendsen, H. J. C.; Postma, J. P. M.; van Gunsteren, W. F.; Dinola, A.; Haak, J. R. Molecular Dynamics with Coupling to an External Bath. *J. Chem. Phys.* **1984**, *81*, 3684–3690.
- (30) Miyamoto, S.; Kollman, P. A. Settle: An Analytical Version of the SHAKE and RATTLE Algorithm for Rigid Water Models. *J. Comput. Chem.* **1992**, *13*, 952–962.
- (31) Hess, B.; Bekker, H.; Berendsen, H. J. C.; Fraaije, J. G. E. M. LINCS: A Linear Constraint Solver for Molecular Simulations. *J. Comput. Chem.* **1997**, *18*, 1463–1472.
- (32) <http://pymol.sourceforge.net>.
- (33) Yerin, A.; Wilks, E. S.; Moss, G. P.; Harada, A. Nomenclature for Rotaxanes and Pseudorotaxanes (IUPAC Recommendations 2008). *Pure Appl. Chem.* **2008**, *80*, 2041–2068.
- (34) Rekharsky, M. V.; Inoue, Y. Complexation Thermodynamics of Cyclodextrins. *Chem. Rev.* **1998**, *98*, 1875–1918.
- (35) Hingerty, B.; Betzel, C.; Saenger, W. Neutron Diffraction of Alpha, Beta and Gamma Cyclodextrins: Hydrogen Bonding Patterns. *J. Biomol. Struct. Dyn.* **1984**, *2*, 249–260.
- (36) Bo, T.; Xu, W.; Jing, W.; Chengguang, Y.; Zhenzhen, C.; Yi, D. Study on the Supramolecular Multirecognition Mechanism of β -Naphthol/ β -Cyclodextrin/Anionic Surfactant in a Tolnaftate Hydrolysis System. *J. Phys. Chem. B* **2006**, *110*, 8877–8884.
- (37) Tanford, C. In *The hydrophobic effect: Formation of micelles and biological membranes*; Wiley-Interscience: New York, 1980; pp 14, 68.
- (38) Wilson, L. D.; Verrall, R. E. A ^1H NMR Study of Cyclodextrin - Hydrocarbon Surfactant Inclusion Complexes in Aqueous Solutions. *Can. J. Chem.* **1998**, *76*, 25–34.
- (39) Hersey, A.; Robinson, B. H.; Kelly, H. C. Mechanism of Inclusion-Compound Formation for Binding of Organic-Dyes, Ions and Surfactants to α -Cyclodextrin Studied by Kinetic Methods Based on Competition Experiments. *J. Chem. Soc., Faraday Trans. 1* **1986**, *82*, 1271–1287.
- (40) Kitano, H.; Okubo, T. Esterolysis in Cyclodextrin-Polyelectrolyte Systems. *J. Chem. Soc., Perkin Trans. 2* **1977**, 432–435.
- (41) Satake, I.; Ikenoue, T.; Takeshita, T.; Hayakawa, K.; Maeda, T. Conductometric and Potentiometric Studies of the Association of α -Cyclodextrin with Ionic Surfactants and their Homologs. *Bull. Chem. Soc. Jpn.* **1985**, *58*, 2746–2750.
- (42) Satake, I.; Yoshida, S.; Hayakawa, K.; Maeda, T.; Kusumoto, Y. Conductometric Determination of the Association Constants of β -Cyclodextrin with Amphiphilic Ions. *Bull. Chem. Soc. Jpn.* **1986**, *59*, 3991–3993.
- (43) Wan Yunus, W. M. Z.; Taylor, J.; Bloor, D. M.; Hall, D. G.; Wyn-Jones, E. Electrochemical Measurements on the Binding of Sodium Dodecyl Sulfate and Dodecytrimethylammonium Bromide with α - and β -Cyclodextrins. *J. Phys. Chem.* **1992**, *96*, 8979–8982.
- (44) Eli, W.; Chen, W.; Xue, Q. The Association of Anionic Surfactants with β -Cyclodextrin. An Isothermal Titration Calorimeter Study. *J. Chem. Thermodyn.* **1999**, *31*, 1283–1296.
- (45) Bravo-Díaz, C.; Gonzalez-Romero, E. Inhibition of the β -Cyclodextrin Catalyzed Dediazoniation of 4-Nitrobenzenediazonium Tetrafluoroborate. Blocking Effect of Sodium Dodecyl Sulfate. *Langmuir* **2005**, *21*, 4888–4895.
- (46) Tang, B.; Wang, X.; Wang, G.; Yu, C.; Chen, Z. Highly Sensitive and Selective Spectrofluorimetric Determination of Tolnaftate through the Formation of Ternary Inclusion Complex of β -Naphthol/ β -Cyclodextrin/Anionic Surfactant System. *Talanta* **2006**, *69*, 113–120.
- (47) Jiang, L.; Deng, M.; Wang, Y.; Liang, D.; Yan, Y.; Huang, J. Special Effect of β -Cyclodextrin on the Aggregation Behavior of Mixed Cationic/Anionic Surfactant Systems. *J. Phys. Chem. B* **2009**, *113*, 7498–7504.
- (48) Guernelli, S.; Laganà, M. F.; Mezzina, E.; Ferroni, F.; Siani, G.; Spinelli, D. Supramolecular Complex Formation: A Study of the Interactions between Beta-Cyclodextrin and some Different Classes of Organic Compounds by ESI-MS, Surface Tension Measurements, and UV/Vis and ^1H NMR Spectroscopy. *Eur. J. Org. Chem.* **2003**, 4765–4776.
- (49) Yu, Y.; Cai, W.; Chipot, C.; Sun, T.; Shao, X. Spatial Arrangement of α -Cyclodextrins in a Rotaxane. Insights from Free-Energy Calculations. *J. Phys. Chem. B* **2008**, *112*, 5268–5271.
- (50) Xing, H.; Xiao, J. Phase Behavior of the Mixed Systems of α -, β -Cyclodextrin and Cationic-Anionic Surfactants. *J. Dispersion Sci. Technol.* **2009**, *30*, 27–32.
- (51) Funasaki, N.; Ishikawa, S.; Neya, S. 1:1 and 1:2 Complexes between Long-Chain Surfactant and α -Cyclodextrin Studied by NMR. *J. Phys. Chem. B* **2004**, *108*, 9593–9598.
- (52) Okumura, Y.; Ito, K.; Hayakawa, R. Theory on Inclusion Behavior between Cyclodextrin Molecules and Linear Polymer Chains in Solutions. *Polym. Adv. Technol.* **2000**, *11*, 815–819.
- (53) Loftsson, T.; Heinsdóttir, D.; Másson, M. The Complexation Efficiency. *J. Inclusion Phenom. Macrocyclic Chem.* **2007**, *57*, 545–552.
- (54) Álvira, E. Mobility of Linear Molecules Inside and Around β -Cyclodextrin. *Mol. Phys.* **2009**, *107*, 1697–1704.
- (55) Okubo, T.; Maeda, Y.; Kitano, H. Inclusion Process of Ionic Detergents with Cyclodextrins as Studied by the Conductance Stopped-Flow Method. *J. Phys. Chem.* **1989**, *93*, 3721–3723.

- (56) Komiyama, M.; Bender, M. L. Importance of Apolar Binding in Complex Formation of Cyclodextrins with Adamantanecarboxylate. *J. Am. Chem. Soc.* **1978**, *100*, 2259–2260.
- (57) Jiang, Y. B.; Wang, X. J. Direct Evidence for β -Cyclodextrin-Induced Aggregation of Ionic Surfactant Below Critical Micelle Concentration. *Appl. Spectrosc.* **1994**, *48*, 1428–1431.
- (58) Xie, J. W.; Huang, D. S.; Xu, J. G.; Chen, G. Z. Room Temperature Phosphorescence Study on Supramolecular System of Cyclodextrin/Surfactants. *Chin. Sci. Bull.* **1997**, *42*, 1468–1472.
- (59) Escandar, G. M.; de la Peña, A. M. Room-Temperature Phosphorescence of 1-Bromonaphthalene upon Formation of β -Cyclodextrin Ternary Complexes with Alcohols and Surfactants: Optimization of Analytical Figures of Merit by Rigorous Equilibrium Studies. *Appl. Spectrosc.* **2001**, *55*, 496–503.
- (60) Saint Aman, E.; Serve, D. A Conductimetric Study of the Association between Cyclodextrins and Surfactants—Application to the Electrochemical Study of a Mixed Aqueous System: Substrate, Cyclodextrin, Surfactant. *J. Colloid Interface Sci.* **1990**, *138*, 365–375.
- (61) García-Río, L.; Leis, J. R.; Mejuto, J. C.; Pérez-Juste, J. Basic Hydrolysis of *m*-Nitrophenyl Acetate in Micellar Media Containing β -Cyclodextrins. *J. Phys. Chem. B* **1998**, *102*, 4581–4587.
- (62) Georges, J.; Desmettre, S. An Electrochemical Study of Mixed Solutions of β -Cyclodextrin and Sodium Dodecyl Sulfate. *J. Colloid Interface Sci.* **1987**, *118*, 192–200.
- (63) MacPherson, Y. E.; Palepu, R.; Reinsborough, V. C. Counterion Binding by Surfactant/ β -Cyclodextrin Inclusion Complexes. *J. Inclusion Phenom. Mol. Recog. Chem.* **1990**, *9*, 137–143.
- (64) Sammalkorpi, M.; Karttunen, M.; Haataja, M. Structural Properties of Ionic Detergent Aggregates: A Large-Scale Molecular Dynamics Study of Sodium Dodecyl Sulfate. *J. Phys. Chem. B* **2007**, *111*, 11722–11733.
- (65) Sammalkorpi, M.; Karttunen, M.; Haataja, M. Ionic Surfactant Aggregates in Saline Solutions: Sodium Dodecyl Sulfate (SDS) in the Presence of Excess Sodium Chloride (NaCl) or Calcium Chloride (CaCl₂). *J. Phys. Chem. B* **2009**, *113*, 5863–5870.

JP103223U